Review

Kushal Sejwal, Mohamed Chami, Paul Baumgartner, Julia Kowal, Shirley A. Müller and Henning Stahlberg*

Proteoliposomes – a system to study membrane proteins under buffer gradients by cryo-EM

DOI 10.1515/ntrev-2016-0081
Received September 12, 2016; accepted December 1, 2016; previously published online January 20, 2017

Abstract: Membrane proteins are vital to life and major therapeutic targets. Yet, understanding how they function is limited by a lack of structural information. In biological cells, membrane proteins reside in lipidic membranes and typically experience different buffer conditions on both sides of the membrane or even electric potentials and transmembrane gradients across the membranes. Proteoliposomes, which are lipidic vesicles filled with reconstituted membrane proteins, provide an ideal model system for structural and functional studies of membrane proteins under conditions that mimic nature to a certain degree. We discuss methods for the formation of liposomes and proteoliposomes, their imaging by cryo-electron microscopy, and the structural analysis of proteins present in their bilayer. We suggest the formation of ordered arrays akin to weakly ordered two-dimensional (2D) crystals in the bilayer of liposomes as a means to achieve high-resolution, and subsequent buffer modification as a method to capture snapshots of membrane proteins in action.

Keywords: buffer gradient; cryo-electron microscopy; image processing; membrane proteins; proteoliposomes.

1 Introduction

Liposomes are colloidal particles formed by one or more bilayers of amphiphillic lipids, and are generally spherical with an aqueous lumen. In medicine, they can be used as potential nanocarriers for the delivery of drugs [1, 2], are foreseen as nanocarriers for functional proteins [3], and are used as detoxification agents [4], to name just a few applications; see Xing et al. [5] for an extensive review. An overview of their use in the field of biosensing is given in Refs. [6] and [7]; in particular, target-specific responsive liposomes have been developed [5]. Liposomes can be used as nanocompartments for crystal growth [2, 8]. Further, some form of liposome container was possibly key to the development of the first primitive cellular systems [9].

Methods to encapsulate different buffers and components within liposomes are well established. It is possible to set up a pH gradient across their bilayer [10], and ion gradients can be used to load liposomes with drugs [1, 10]. Compatible with a possible role in evolution, the spontaneous encapsulation and concentration of biological macromolecules (protein macromolecules, ferritin, and ribosomes) and the encapsulation of an entire minimal protein synthesis system have also been reported, and protein synthesis was demonstrated (reviewed in Ref. [9], see also Ref. [11]).

Proteoliposomes are unilamellar liposomes with proteins inserted in their lipid bilayer. They offer an additional level of complexity and can serve as model systems for biological membranes. Proteoliposomes can be formed by removing the detergent from solubilized lipid/membrane protein mixtures or from mixtures of detergent-solubilized membrane proteins and preformed liposomes ([12, 13]; details below), are often formed together with planar two-dimensional (2D) crystals (membrane proteins incorporated as regular arrays in a planar lipid bilayer) in 2D crystallization experiments [14], and can occur in cell-free protein synthesis (CFPS) experiments when liposomes are present [15]. Various methods have been applied to monitor the reconstitution of membrane proteins into liposome bilayers (e.g. light scattering [16], dual-color fluorescence cross-correlation spectroscopy using green-labeled membrane protein and red-labeled liposomes [17]), to determine the orientation of the protein in the lipid bilayer [18–20], and to follow the effect that protein insertion has on the lipids present (e.g. fluorescence anisotropy [21]). Proteoliposomes are used to investigate and

***Corresponding author: Henning Stahlberg,** Center for Cellular Imaging and NanoAnalytics (C-CINA), Biozentrum, University of Basel, Basel 4056, Switzerland, e-mail: henning.stahlberg@unibas.ch.
http://orcid.org/0000-0002-1185-4592
Kushal Sejwal, Mohamed Chami, Paul Baumgartner, Julia Kowal and Shirley A. Müller: Center for Cellular Imaging and NanoAnalytics (C-CINA), Biozentrum, University of Basel, Basel 4056, Switzerland

demonstrate the function and activity of membrane proteins, e.g. by the presence or development of ion concentration gradients across the bilayer ([22], reviewed in Refs. [13, 23]). They have also been used in structural studies carried out by cryogenic electron microscopy (cryo-EM; details are below) and by solid-state nuclear magnetic resonance (NMR [24]). The latter avoids the use of cryogenic procedures but is restricted to relatively small membrane proteins, and these have to be present at relatively high concentrations.

Electron microscopy, particularly cryo-EM, is routinely used to characterize liposomes and proteoliposomes [25]. Negative stain transmission electron microscopy (TEM) can clearly reveal membranes and liposomes, especially when the negative stain is phosphotungstic acid, and gives information about sample homogeneity (resolution ~ 20 Å [26, 27]). It is also used to screen for 2D membrane protein crystals in crystallization trials and to assess their quality and characterize them as planar, tubular, or vesicular [28, 29]; vesicular 2D crystals is an alternative name for proteoliposomes with 2D crystals in their bilayer. Before cryo-EM was fully established, high-quality negatively stained samples were analyzed further by helical analysis (tubular crystals) or electron crystallography (flat crystalline sheets or planar crystalline regions of collapsed vesicles) [30]; the formation of vesicular 2D crystals allowed corresponding activity assays to be made [31]. Freeze-fracture electron microscopy, where the fracture plane that follows the bilayers of liposomes or membranes is replicated for imaging, reveals the inner/outer surface structure of this layer and the presence of proteins, although at resolutions typically below 3 nm [32]. Cryo-EM, in which liposomes are flash-frozen in buffer and imaged at cryogenic temperatures ([33]; details are below), gives a more precise view of their bilayer that allows the membrane thickness to be measured and, especially when combined with electron tomography (ET; resolution >10 nm [34]), reveals their three-dimensional (3D) shape in solution and the location and shape of any electron-dense material present [35]. As well as to characterize the morphology, size, and shape of liposome samples, cryo-EM can be used to visualize the effect of additives [36], encapsulation ([2] addressed below) and internalization [37] phenomena, and protein-liposome interactions [3, 38–41]. Further information about the use of cryo-EM to characterize lipid-based and other nanoparticles can be found in a recent review by Stewart [42].

In this article, we consider the role of membrane proteins, and outline methods used to insert purified membrane proteins into the bilayer of unilamellar liposomes and the use of cryo-EM to characterize liposomes and proteoliposomes. We discuss the possible use of proteoliposomes and cryo-EM to capture snapshots of membrane proteins "in action" under close-to-native conditions and reveal the conformational changes that take place.

2 Membrane proteins and the importance of the lipid bilayer

Genome-wide sequence studies predict that about one-third of all expressed human gene products are integral α-helical membrane proteins [43]. Membrane proteins can be densely packed in biological membranes. For example, mitochondrial membranes are reported to have a lipid-to-protein ratio (w/w) of 1 or less [44]. The updated version of the Singer-Nicolson model describing the structure and function of cell membranes [45] underlines the important role of the proteins they contain. Several transmembrane proteins present in the lipid bilayer of a cell membrane perturb it, influence its thickness and curvature, and interact with one another restricting fluidity. Membrane proteins also mediate various vital processes in the biological membranes of cells and organelles, such as energy transport during photosynthesis or respiration, transport of molecules across the membranes, transmission of chemical signals, anchoring of the cytoskeleton, and catalysis of chemical reactions. The pivotal role of membrane proteins in cellular function explains their high medical importance. It is estimated that more than 50% of all available drugs act on membrane proteins [46]. Despite their importance, however, structural studies remain challenging, as evident from the fact that only approximately 3% of all the known structures published in the protein data bank (PDB) are of membrane proteins (http://www.rcsb.org/pdb, as of September 2016).

Compared to cytoplasmic proteins, it is difficult both to purify membrane proteins in sufficient amounts for X-ray crystallography studies and to obtain well-diffracting 3D crystals. Electron crystallography of membrane proteins reconstituted in a planar lipid bilayer as 2D crystals has long been an alternative approach [47–49]; it requires much less material and the proteins are imaged while embedded in a lipid bilayer. Proteoliposomes offer the possibility of going a step further and imaging membrane proteins in the presence of a membrane potential or ligand gradient [50], but this has not been demonstrated experimentally.

The importance of the lipidic membranes and their surface, transmembrane, and dipole potentials for membrane protein aggregation, conformation, and function,

is becoming increasingly clear [51]. As a consequence, the need to determine the structure of membrane proteins in a "close-to-native" environment is now apparent. The surface potential [52] generated by the lipid headgroups changes the concentration of ions close to the membrane surface and ion uptake. The dipole potential (+200 mV to +500 mV or more) arises from the alignment of dipolar residues and water within the membrane. It depends on the structure of the lipids and affects ion permeability within and in the proximity of the membrane. The transmembrane potential (typically −40 to −120 mV) depends on the ion concentrations on either side of the membrane. Variations in the membrane voltage trigger the function of some membrane proteins. For example, a change in the transmembrane potential causes voltage-gated channel proteins to undergo a conformational change, which can lead to opening of the channel pore and conduction of ions [53].

3 Liposome preparation

We discuss two ways to prepare liposomes below (Figure 1). Other methods are reviewed in Refs. [54, 55] (less conventional methods) and in Ref. [56] (microfluidic approaches).

3.1 Film dispersion method

Lipids solubilized in chloroform (typical concentration, 10–25 mg/ml) are transferred to a glass tube or flask. A stream of argon gas is passed over the solution to evaporate the solvent. A film of lipids forms on the walls of the tube. Residual solvent is removed under vacuum (e.g. by active pumping at 5–15 mbar for a few hours). A rotary evaporator, also known as a "rotavap", can also be used [57]. Afterwards, the lipid film is dispersed in the desired aqueous buffer or buffer plus additives (e.g. for encapsulation experiments) by adding liquid and vortexing until no film is visible on the vessel walls. When working with phospholipids, this generally results in the spontaneous formation of multilamellar vesicles (MLV) and large unilamellar vesicles (LUV). This procedure should be extended by an extrusion step (e.g. Mini-Extruder device, Avanti Polar Lipid Inc., USA) if small unilamellar vesicles (SUV) are required and, if necessary, followed by size exclusion chromatography to obtain more homogeneous size distributions (see below).

3.2 Dialysis method

In this case, the lipid film is solubilized in approximately 1 ml of buffer containing detergent at a concentration

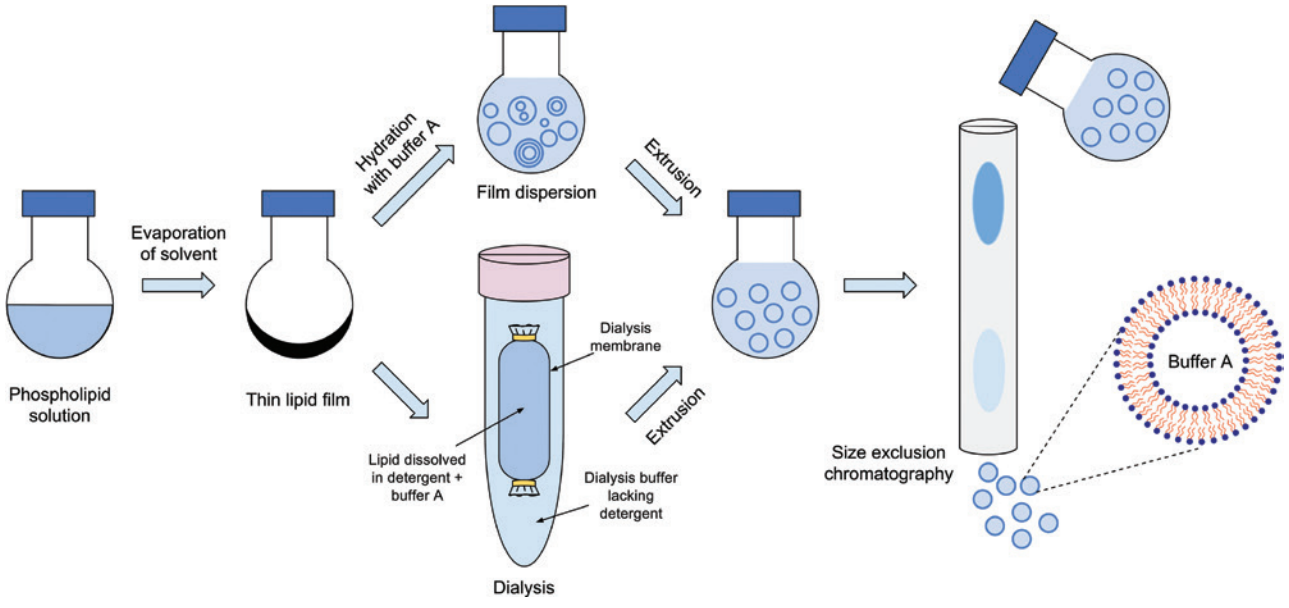

Figure 1: Liposome formation by the film dispersion and dialysis methods. The extrusion step promotes the formation of unilamellar liposomes of uniform size. Size exclusion chromatography decreases the size variation and can be used to exchange the dispersion buffer. The liposomes shown in Figures 3–6 and employed to obtain the proteoliposomes shown in Figure 7 were prepared by the film dispersion method and manually extruded 11 times through a polycarbonate filter (pore size of 100 or 200 nm) using a mini-extruder (Avanti Polar Lipid Inc., USA).

well above the detergent's critical micellar concentration (cmc), loaded into dialysis buttons (e.g. Hampton dialysis buttons, Hampton Research, Aliso Viejo, CA, USA) or a dialysis bag and dialyzed against detergent-free buffer for hours to weeks, depending on the type of detergent used and its cmc. Liposomes form as the detergent concentration falls below the cmc. The method is assessed in Ref. [12]. Following dialysis, the liposome mixture generally has to be extruded multiple times through a filter using a mini-extruder (AvantiPolar Lipid Inc., USA) to obtain homogeneous unilamellar vesicles.

Extrusion helps to maintain a uniform liposome size distribution and favors the formation of unilamellar vesicles [58, 59]. The average size and the size distribution of the liposomes depend on the pore size of the filter and on the lipid composition [60]. A detailed description of the method can be found in the study by Mull et al. [61]. The size distribution can be decreased by a subsequent size exclusion chromatography step, which is also a convenient way to exchange the dispersion buffer for encapsulation experiments (see below). In this context, it is important to note that extrusion and the type of filter used can influence the results of encapsulation experiments, as demonstrated by Colletier et al. [62].

The preparation of GUVs is described in detail in Ref. [63]. Liposome formation by gentle dilution and electroformation methods are also described in Ref. [64].

4 Reconstitution of membrane proteins

Reviews by Stockbridge et al. [65] and Rigaud and Levy [12] give detailed accounts of the reconstitution of membrane proteins into liposomes and also consider the overall characterization of the resulting proteoliposomes [12] and their use for activity measurements [65].

There are two basic approaches to reconstitution. One is detergent-mediated, as detailed below for 2D crystals. The other is a variation where preformed liposomes are used as a starting point instead of detergent-solubilized lipids. The use of preformed liposomes is reported to favor unidirectional insertion of the membrane proteins [12]. In addition, Rigaud et al. employed a "step-by-step" method to understand the mechanisms governing protein reconstitution, assuming that assembly mirrors disassembly (summarized in Ref. [12]). In this approach, the solubilization of preformed liposomes is characterized by the stepwise addition of detergent. Protein is then added at each well-defined step to determine the best reconstitution conditions.

To obtain highly ordered 2D crystals, detergent-solubilized purified membrane proteins in buffer solution are mixed with detergent-solubilized lipids and the amount of detergent is reduced slowly by dialysis (Figure 2A) [66], more rapidly by the use of Biobeads [67], by the addition

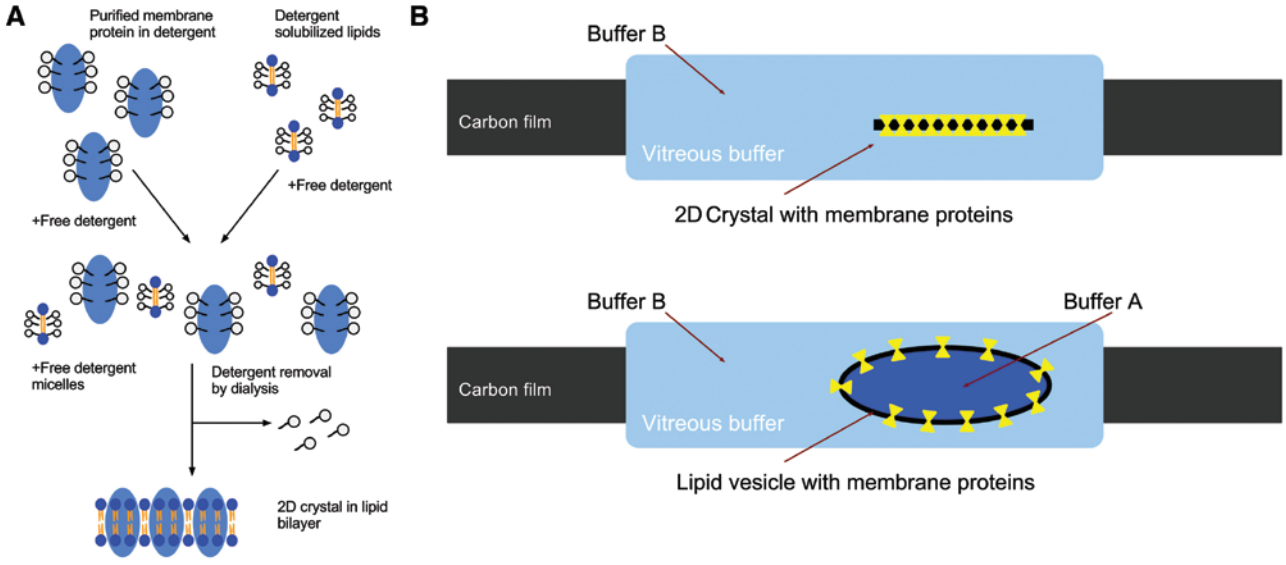

Figure 2: Reconstitution of membrane proteins in a lipid bilayer and vitrification for cryo-EM. (A) The principle of 2D crystallization: detergent-solubilized and purified membrane proteins are mixed with detergent-solubilized lipids, and the detergent is removed to form 2D crystals. (B) Vitrification of planar 2D crystals (above) and proteoliposomes with 2D crystals in their bilayer (below). The proteoliposomes can encapsulate one buffer system and be dispersed in another, as indicated. The ion or ligand gradient across their bilayer is experienced by the reconstituted membrane proteins.

of cyclodextrin [68], or by gradual dilution [16]; for further details, see Ref. [69]. In all cases, many conditions have to be screened to find the conditions (detergent, buffer, pH, additional salts, lipid-to-protein ratio, temperature gradients, time scale) that lead to the best well-ordered planar 2D crystals [69] or to helical tubular crystals [70, 71]. The latter are often open at one or both ends, which does not allow a buffer gradient to be set up across the lipid bilayer. High-quality samples can be vitrified or embedded in sugar solution (such as trehalose) and vitrified and imaged by cryo-EM [72]. Computational image processing of the micrographs and diffraction data [49, 69, 73–75] is then utilized to reconstruct the 3D structure of the protein at high resolution.

In practice, a mixture of planar 2D crystals or helical tubular crystals and liposomes of various types – pure lipid, packed to different degrees with protein, sometimes with 2D crystals in their bilayer – is often obtained in 2D crystallization runs. The ratio of these, the stoichiometric ratio of the components present in 2D crystals, and the crystal form obtained, depend on the membrane protein, lipids, and crystallization conditions.

Potentially, cell-free protein expression offers a completely different yet related approach to membrane protein reconstitution for structural studies. CFPS systems exploit the transcription and translation machinery used by cells to express soluble and membrane proteins *in vitro* [76, 77]. The additional presence of pre formed liposomes in the system has been shown to increase the cell-free expression and solubility of diverse aggregation-prone α-helical membrane proteins [78], and the insertion of membrane proteins directly into liposomes during production to produce functional proteoliposomes has been demonstrated in a number of cases [15]. In their review, Katzen et al. [79] state that the heterogeneity of such samples makes them unsuitable for structural biology. It remains to be seen whether the possibility to obtain essentially monodisperse liposome preparations by a DNA template method [80] will change this situation.

It is known that the insertion of a membrane protein into liposomes can require the presence of a particular lipid [81] and that lipids can influence the aggregation state of membrane proteins in the bilayer [82]. A close interaction between membrane proteins and specific lipids has been described [30, 83]. The many physicochemical properties of lipids and lipid membranes that can influence the activity of membrane proteins are detailed in Sachse et al. [15]; some aspects were already discussed above [51]. Further information relevant to the reconstitution of functional membrane proteins can be found in Ref. [84].

5 Cryo-EM methods

To prepare samples for cryo-EM imaging, a few microliters of sample are pipetted onto cryo-EM grids that are covered with a holey carbon film that was previously made hydrophilic by glow discharge in a low pressure of air. The grids are then blotted with filter paper and rapidly plunge-frozen in liquid ethane cooled by liquid nitrogen; both of these steps can be performed using a dedicated instrument (e.g. an FEI Vitrobot or Leica GP plunger). Afterwards, a vitreous sample layer fills the holes of the carbon film (Figure 2B). The blotting conditions and the grid's surface properties with respect to the sample determine the shape and thickness of the layer, making it thinner at the center of holes in a hydrophilic carbon film. The frozen grids can be stored or immediately transferred to a cryo-holder, inserted in the cryo-EM instrument, and imaged.

There are, of course, variations to this protocol. In one, a thin continuous layer of carbon, graphene or graphene oxide [85–87] is placed on top of the thicker holey carbon film and the sample is deposited on top of it. This method is useful when proteins tend to adhere to the thick carbon at the edge of holes rather than distribute in the vitreous ice within them, and is also used to prepare 2D crystals for imaging and electron crystallography. Grids holding 2D crystals are also prepared by the so-called back-injection and sandwich methods. In the former, the 2D crystals on the grid are embedded in a sugar layer, blotted, and plunge-frozen. In the latter, the 2D crystals are sandwiched between two thin carbon layers, and excess sample is removed by blotting from the side before the grid is plunge-frozen.

In all of the above cases, the paper-blotting step removes over 99.99% of the sample volume and can affect its quality. More economical methods in terms of sample loss are being developed, such as the use of nanoliter droplet deposition on self-blotting grids [88] or the direct deposition of nanoliter sample volumes via microfluidic devices [89].

For structural studies, the transmission electron microscope is usually operated at 100 to 300 kV and micrographs are recorded at a range of defocus settings under low electron-dose conditions to minimize beam damage. The magnification employed is sample-dependent. Detectors vary, CCD cameras being used for screening runs. Direct electron detectors deliver the highest contrast and resolution and support "movie-mode" imaging where a series of frames are recorded at very low dose and summed to give the final image [90]. This allows correction to be made for sample drift by dedicated software

such as *Motioncorr* [90], *Unblur* [91], or *Zorro* [92] before the averaging step.

As purified proteins usually orient in different ways in the vitreous buffer film, their 3D structure can be directly reconstructed by "single particle analysis" of the 2D projections obtained [93]. By contrast, 2D crystals (Figure 2B, top) only present one view of the protein to the beam and have to be tilted to obtain 3D information. As the tilt angle is limited (generally to ±60°), this results in a so-called missing cone and, as a consequence, the structures reconstructed from the images tend to have a lower resolution in the z-direction [49]. Crystalline samples are also examined in diffraction mode and analyzed by electron crystallography software, as outlined in Abeyrathne et al. [69]. The missing phase information is obtained from images.

The same grid preparation procedure can be used when cryo-electron tomography (cryo-ET) is employed to look at liposomes and proteoliposomes (Figure 2B, bottom). However, samples generally have to be thinner than 500 nm to ensure that the number of transmitted electrons is sufficient for imaging. Thicker samples would have to be rapidly frozen at high pressure, which might necessitate additional steps (fixation and freeze substitution), and cut into serial sections at cryogenic temperatures [94]; the sections can then be mounted on TEM grids for inspection. In both cases, the vitrified sample has to be tilted in the beam for imaging and, as with 2D crystals, there is the problem of a missing wedge or cone in Fourier space. As the electron dose has to be limited to avoid sample damage, the signal-to-noise ratio of the tomograms is low. Thus, while larger features can be immediately recognized, subtomogram averaging [95, 96] is required to reveal smaller macromolecules.

An assessment of negative stain TEM and the various cryogenic methods can be found in the study by Thompson et al. [97].

Figures 3–7 illustrate cryo-EM imaging of liposomes and proteoliposomes. These images were not published before. Grids were prepared by pipetting 4 µl of the liposome or proteoliposome sample onto glow-discharged, holey carbon films (Quantifoil R2/1, Quantifoil Micro Tools, Jena, Germany). Grids were blotted and rapidly plunge-frozen in liquid ethane cooled by liquid nitrogen by using a MarkIVVitrobot (FEI, Eindhoven, The Netherlands) with a fast blotting time of 1 s and a blotting force of 1. They were transferred to a Gatan-626 cryo-holder for imaging. The micrographs were recorded under low-dose conditions (25 electrons/Å^2) on a CM200 transmission electron microscope (FEI Company, Eindhoven, The Netherlands) equipped with a TVIPS F416 CMOS camera (TVIPS, Gauting, Germany). The accelerating voltage was 200 kV, and the nominal magnification was 50,000×. The defocus settings employed were chosen so that the lipid bilayer of the liposomes could be distinguished in the micrographs.

6 Characterization of liposomes and proteoliposomes by cryo-EM methods

Cryo-EM can be used to characterize and control the quality of liposome samples [80], including those that are foreseen for use in biomedicine and nanotechology [2, 3, 100, 101]. It also gives detailed information about encapsulation and internalization phenomena, revealing the location of the proteins (Figure 6) or nanoparticles [2, 102]. Depending on their nature and the experimental conditions, nanoparticles can reside in the liposome lumen [37] or between the two leaflets of the lipid bilayer [35]. Cryo-ET is used to examine liposomes [37, 39] and proteoliposomes [103] as well as native cell membranes [104] and cells [105], and to determine the localization and structure of proteins complexes [106] within them, or to follow interactions with external agents such as viruses [107, 108]. Cryo-ET combined with sub-volume averaging is able to reach very high resolution on membrane-embedded structures [109], but this is still rarely achieved in practice. However, even with lower resolution data, such studies help to understand how complex nanomachines might influence membranes *in vivo* [103, 110].

As with all methods, misleading artifacts can occur. In cryo-EM, these are caused by the vitrification process and variations in the thickness of the vitrified sample layer. Three common problems are mentioned here. First, variations in the thickness of the vitrified layer can effectively sort the liposomes by size, concentrating larger liposomes in thicker regions and giving a misleading impression of the sample. Second, when the vitreous layer is too thin, liposomes protrude from it and the exposed region collapses, resulting in increased contrast in the corresponding area of the 2D projections (Figure 3A, right). Third, some liposomes may deform during cryo-EM grid preparation, which could be caused by drying of the sample solution and the accompanying increase in salt concentration and osmolarity or by the surface tension of water flattening and sometimes also breaking them. Further possible effects are outlined in Almgren et al. [25].

Because almost all of the liquid deposited on the EM grid is removed by a paper-blotting step before vitrification, only a qualitative impression of the sample can be

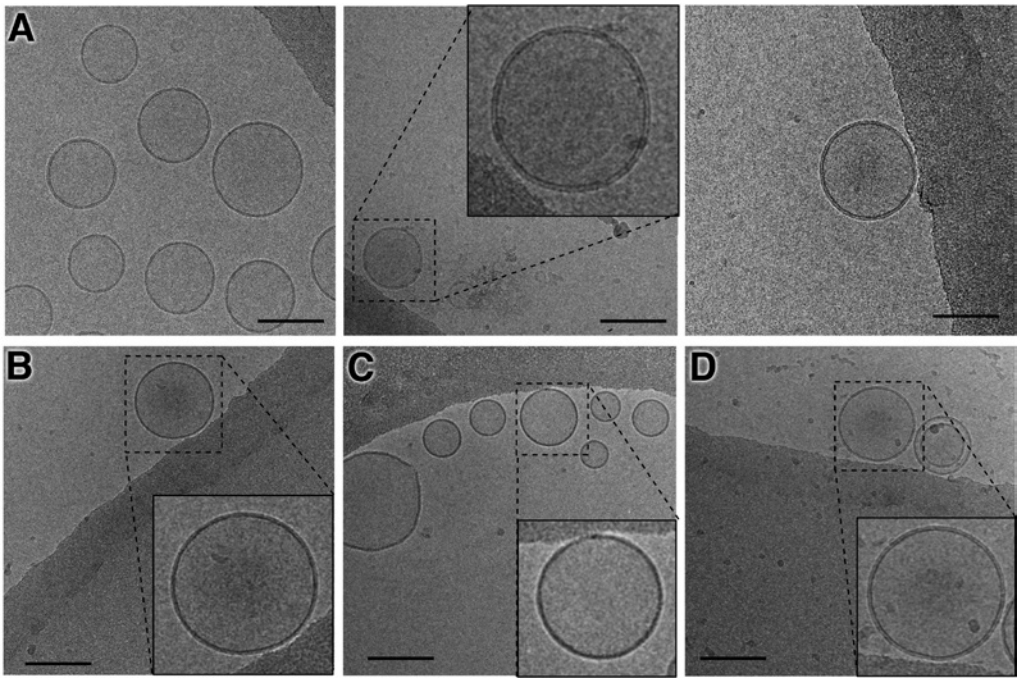

Figure 3: Encapsulation of fluorescent dye and heavy metal chemicals investigated by cryo-EM. (A) Control. *E. coli* polar lipid extract liposome with the same buffer system (20 mM Tris-HCl pH 7.6, 1 mM EDTA) on both sides of the bilayer. Under these conditions, the image contrast and noise distribution should be uniform inside and outside of the liposome (left and center). The two leaflets of the lipid bilayer can be distinguished (inset). A contrast gradient in the liposome lumen that increases towards the center indicates that the liposome protruded from the vitrified layer and collapsed (right), i.e. it is a grid-preparation artifact. (B–D) Encapsulation. *E. coli* polar lipid extract liposomes were formed in 20 mM Tris-HCl pH7.6, 1 mM EDTA buffer, containing the indicated additional component and dispersed in the same buffer without it. (B) The fluorescent dye CF, 100 mM. (C) CsCl, 100 mM. (D) $FeCl_3$, 100 mM. Encapsulation could not be visualized by cryo-EM. The increased contrast towards the center of liposomes shown in B and D is a grid preparation artifact, as discussed in (A). Insets: magnified views of the indicated liposomes. Equivalent results were obtained with DMPC liposomes under the same buffer conditions. Scale bars: 100 nm.

obtained by cryo-EM; the assumption is made that blotting has no effect on sample composition or appearance. For this to be true, the humidity and temperature within the blotting apparatus have to be finely tuned to avoid drying or swelling of the sample during or shortly after blotting, which would change the salt concentration and osmotic pressure. The absolute determination of, e.g. the mean liposome diameter or the relative occurrence of different liposome species in the sample, is not possible. Ideally, quantitative answers that can be used for statistical analysis would be required, e.g. to determine the stabilizing effect of modified lipids and different bilayer compositions [36, 111] or the suitability of a formulation for drug delivery [3, 100]. Thus, at present, cryo-EM has to be combined with other methods (e.g. photon correlation spectroscopy was employed by Menzel et al. [111]). The recent development of a microfluidic platform capable of cryo-EM grid preparation in a loss-less manner [89] promises to change this situation in the near future, as the newly developed methods do not involve any paper-blotting. However, as with conventional methods, the presence of sample on electron-opaque regions of the grid (grid bars, thick carbon of theholey carbon film) cannot be avoided.

7 Determination of membrane protein structure by cryo-EM

Single particle cryo-EM can be used to determine the structure of membrane proteins solubilized in detergent [112] or other surfactants (reviewed in Ref. [113]), including nanodiscs [114] and amphiphols [115]; reviewed in detail in Ref. [116]. Alternatively, membrane proteins can be crystallized in 2D in a planar lipid bilayer and examined at cryogenic temperatures by electron crystallography [69].

The high-resolution structural analysis of proteins reconstituted in the non-planar bilayer of a liposome is

challenging. The random spherically constrained (RSC) single particle reconstruction method [117, 118] can be applied to spherical unilamellar proteoliposomes that are sparsely populated with proteins and tethered to a 2D streptavidine crystal (~2-nm resolution structure of the BK potassium channel [118]) or adsorbed directly to a thin carbon film [119], and particles can be identified in the images by automated procedures (e.g. [119]). In this work, particles were identified in liposomes after image subtraction of the underlying streptavidin 2D crystal (if present) and of the liposome bilayer. Another approach requires the formation of membrane protein/lipid polyhedral nanoparticles [120]. These symmetric liposomes can then be analyzed by cryo-ET and single particle cryo-EM. The structure of the mechanosensitive channel protein was solved at ~1-nm resolution by this method, but although comparable liposomes were obtained with two other proteins, it remains to be seen how generally applicable it is.

The structure of bovine F_0F_1 ATPase in a lipid membrane was determined at a resolution of 24 Å from vesicular 2D crystals using a combination of cryo-ET, subtomogram averaging, and electron crystallography of 2D tomographic slices [103]. This was facilitated by the fact that the vesicles were flat and relatively thin rather than spherical, as the F_0F_1 ATPases on opposite sides of them interacted via their rotor rings.

Cryo-ET and subtomogram averaging were also recently used to determine the structure of the mouse serotonin 5-HT3 receptor densely packed in the bilayer of liposomes. The 12 Å resolution achieved revealed secondary structural elements and showed that the short horizontal helices take part in receptor-receptor interactions in the bilayer [121].

8 The use vesicular 2D crystals and cryo-EM to structurally characterize membrane proteins in action

Although the sheet-like 2D crystals employed for cryogenic electron crystallography provide a more native lipidic environment for the membrane protein than 3D crystals, their surroundings do not mimic the conditions present on either side of native membranes; the membrane proteins in single flat crystalline sheets or open-ended helical tubes experience the same buffer on both sides (buffer A in Figure 2B). The typical salt, pH, and ligand concentration gradients that occur across the membranes of cells and organelles are not present and cannot be generated. However, vesicular 2D crystals would allow such gradients to be created, at least for a short period of time.

As outlined above, a few cryo-EM studies have been made using proteoliposomes without a gradient across the bilayer, giving membrane protein structures at resolutions of typically 1–2 nm [121]. The method now proposed here is to form unilamellar liposomes in buffer A, which then encapsulate that buffer in their lumen, and reconstitute the membrane protein into the liposome bilayer using the same buffer, at the same time achieving some 2D crystalline arrangement of the membrane proteins in the bilayer. The outer buffer of this suspension of semi-crystalline proteoliposomes can then be exchanged to buffer B, and the structure of the reconstituted membrane proteins can be determined by cryo-EM and electron crystallography (Figure 2B). As noted above, the use of preformed liposomes will favor the unidirectional insertion of the membrane protein. After buffer exchange, buffer A must remain encapsulated within the proteoliposomes for a period of time, during which the membrane proteins experience different environments on either side of the lipid bilayer and sample grids can be flash-frozen for cryo-EM. Imaging will then deliver a "snapshot" of the membrane protein in action, allowing the conformational changes involved to be elucidated. In its simplest form, this procedure would mean adding a ligand to either buffer A or buffer B (also suggested by Jiko et al. for the F_0F_1 ATPase vesicles they generated [103]), followed by imaging or protein activity tests. Samples containing membrane proteins in a 2D crystalline arrangement within liposomes have been used for activity studies [31]. The use of densely crowded 2D crystal arrays instead of proteoliposomes with only a few membrane proteins will facilitate structural analysis by cryo-EM, by greatly reducing the number of images required. Further, this method is expected to deliver higher resolution if the advantages of single particle analysis and electron crystallography can be merged (discussed below).

The liposomes and proteoliposomes generated must have the following three important properties: (i) They must retain the encapsulated content. (ii) They should not burst or contract due to osmotic pressure. (iii) They must withstand vitrification for cryo-EM.

The cryo-EM images shown in Figures 3–6 document experiments carried out to assess the extent to which cryo-EM can be used to monitor the encapsulation of various chemicals, proteins, and gold markers by liposomes formed from either *E. coli* polar lipid extract or the synthetic zwitterionic lipid, 1,2-dimyristoyl-sn-glycero-3-phosphocholine (DMPC). To confirm encapsulation, the lumen of liposomes encapsulating material must

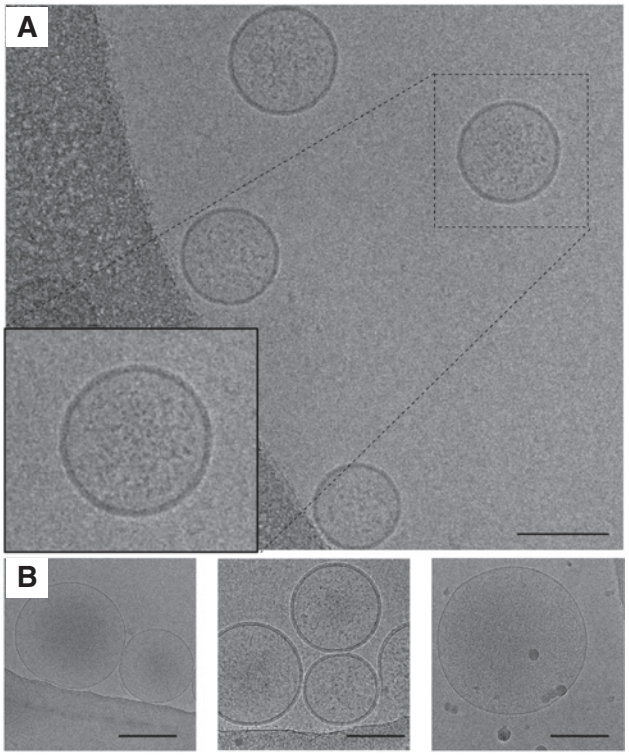

Figure 4: Cryo-EM images of liposomes encapsulating bovine serum albumin (BSA). *E. coli* polar lipid extract liposomes were formed in 20 mM Tris-HCl pH 7.6, 1 mM EDTA buffer containing the indicated amount of BSA and dispersed in the same buffer without it. (A) BSA, 33 mg/ml. (B) BSA, 5 mg/ml (left), 10 mg/ml (middle), 50 mg/ml (right). The concentration of BSA in the starting buffer had to be 10 mg/ml or more for encapsulation to be visible. Scale bars: 100 nm.

display either uniform higher contrast than the dispersion buffer (background contrast) or a different morphology. In the examples shown, size exclusion chromatography was employed to remove non-encapsulated material from the samples after encapsulation, unless otherwise stated. When 100 mM 5(6)-carboxyfluorescein (CF; $C_{21}H_{12}O_7$; a florescent dye), cesium chloride (CsCl), or ferric chloride ($FeCl_3$) was present in the encapsulation buffer, the only contrast differences observed within the liposomes were grid preparation artifacts that could be misleading to the inexperienced eye (Figure 3B–D; compare with A). These are due to the collapse of liposome regions that protrude from the vitreous buffer layer. The electron scattering power and concentration of CF, which is membrane impermeant, was too low for this molecule to be detected in the lumen of liposomes after buffer exchange. Similarly, CsCl and $FeCl_3$ could not be detected and, as for CF, this was independent of the lipid used. The result can be understood in the light of the following: first,

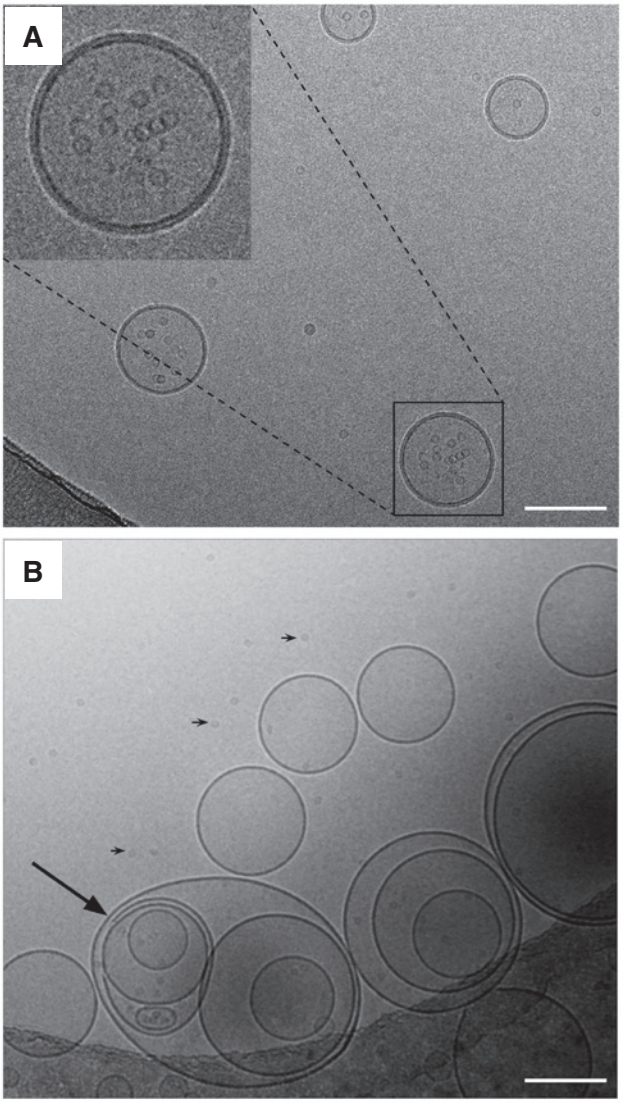

Figure 5: Encapsulation of apoferritin and urease investigated by cryo-EM. *E. coli* polar lipid extract liposomes were formed in 20 mM Tris-HCL pH 7.6, 1 mM EDTA buffer containing the indicated additional component and dispersed in the same buffer without it. (A) Apoferritin, 2 mg/ml. Some liposomes contained apoferritin and retained it when the buffer was exchanged by size exclusion chromatography. In some cases, the amount was more than expected from the distribution of apoferritin at the same concentration in the same buffer without lipids. This might be caused by spontaneous encapsulation as reported for ferritin [9]. The few apoferritin complexes in the background of the image are probably from liposomes that opened during the size chromatography or vitrification steps. (B) Urease, 3.5 mg/ml. Encapsulation was probably not successful. After size exclusion chromatography, the distribution of urease in the background (small arrows) and apparently in the lumen of liposomes is essentially the same. The later might be in the vitreous buffer above and below the liposome imaged, or indeed inside it. Only the small oval liposome (large arrow) looks as if it might contain encapsulated protein. Scale bars: 100 nm

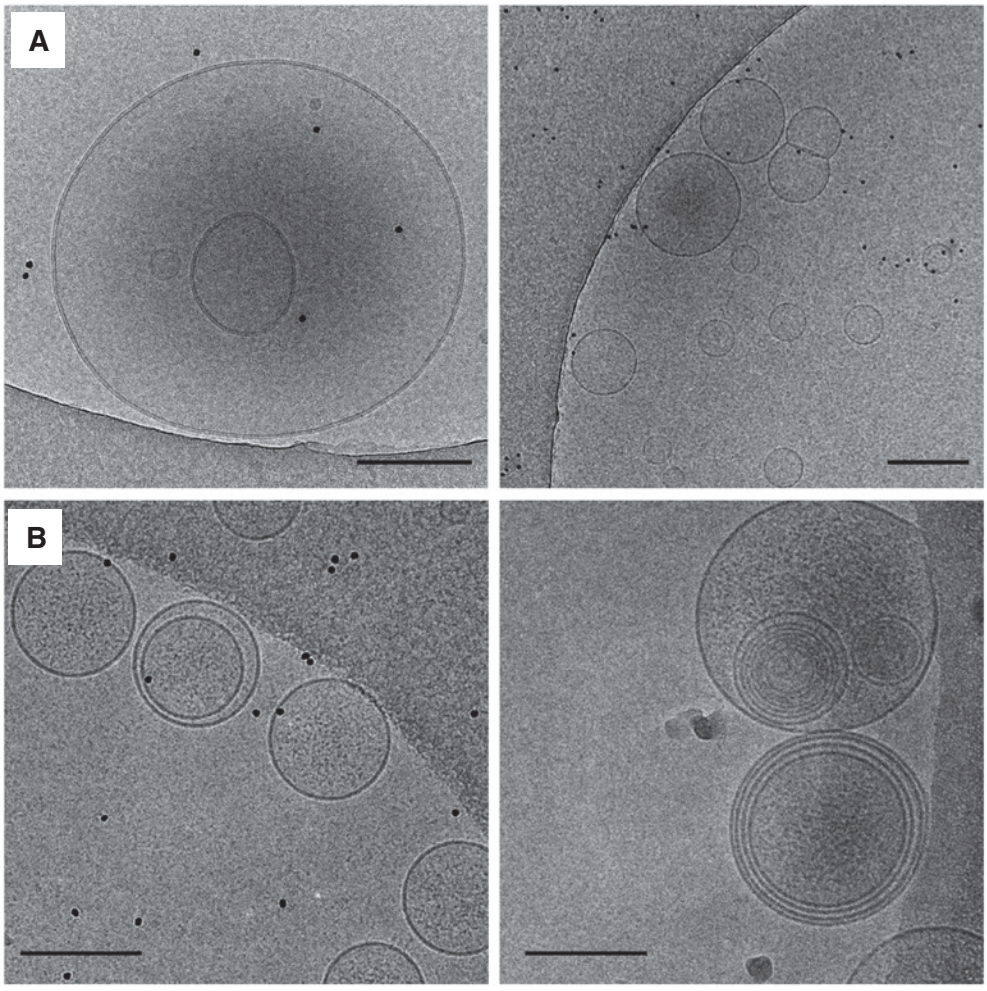

Figure 6: Encapsulation of gold nanoparticles (GNPs) investigated by cryo-EM. *E. coli* polar lipid extract liposomes were formed in 20 mM Tris-HCl pH 7.6, 1 mM EDTA buffer containing the indicated additional material and dispersed in the same buffer without it. (A) GNPs, diluted 1 : 60 in the same buffer. The distribution of GNPs in the background and apparently in the lumen of the liposomes is the same before (left) and after (right) ultracentrifugation, showing that ultracentrifugation could not be used to remove non-encapsulated material in this case. (B) GNPs, diluted 1 : 60 in the same buffer and BSA, 33 mg/ml, before (left) and after (right) size exclusion chromatography using a 1.5 × 10 cm Econo-Column (Bio-Rad) packed with G-25 resin (Sigma-Aldrich) equilibrated with 20 mM Tris-HCl pH 7.6, 1 mM EDTA; the GPNs were removed by the chromatography step. Thus, GPNs were not successfully encapsulated. The patterning/increased contrast associated with encapsulated BSA can be distinguished (compare with Figure 4). See main text for details. GNPs (diameter, 5 nm) were purchased from Cell Microscopy Core at the University Medical Centre in Utrecht, The Netherlands. They were conjugated with protein A-Gold (PAG), and were supplied in phosphate-buffered saline (PBS) buffer containing 12–15% glycerol, 0.1% BSA, and 0.02% sodium azide. Scale bars: 100 nm.

Garcia-Manyes et al. showed that the zeta-potential of a DMPC unilamellar liposome dispersion decreases as the ionic strength of the solution is increased and concluded that cations adsorb to the lipid headgroups at the surface of the bilayer [122]. Second, in de-ionized water, the encapsulation of Fe^{2+} ions by liposomes composed of 80% (mol/mol) egg lecithin, 10% (mol/mol) cholesterol, and 10% (mol/mol) Tween 80 is less at higher concentrations, i.e. at higher ionic strength, and is increased by the presence of chelating agents [123]. Thus, the amount of Cs^+ and Fe^{3+} ions encapsulated in the DMPC or *E. coli* polar lipid extract liposomes used here might have been increased by decreasing the CsCl and $FeCl_3$ concentrations used and increasing the concentration of the chelating agent EDTA in the buffer solutions; the encapsulation of chelated Cs^+ and Fe^{3+} might have been favored.

The protein bovine serum albumin (BSA; 66.5 kDa; diameter is around 7 nm) was encapsulated, remained encapsulated during the chromatography step, and was visible in the lumen of the liposomes formed by *E. coli* polar lipid extract (Figure 4). The same result was obtained when the encapsulation of apoferritin (~ 480 kDa; diameter, 12 nm

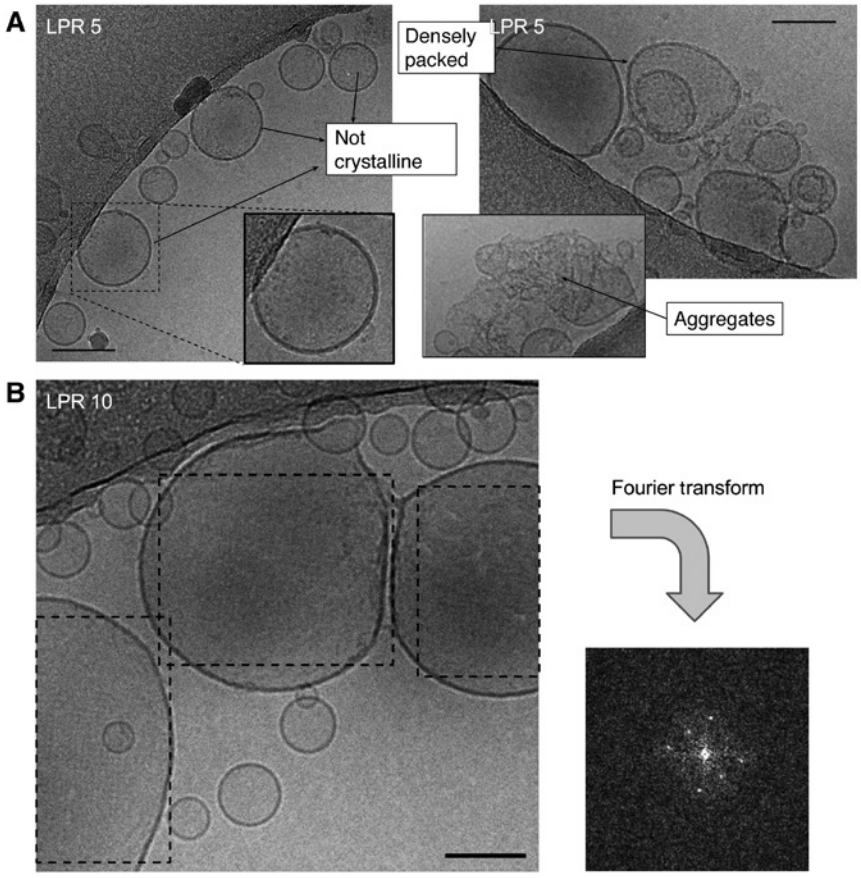

Figure 7: Cryo-EM images of liposomes reconstituted with the potassium channel MloK1. In the crystallization screens, liposomes from *E. coli* polar lipid extract preformed by the film dispersion method and dispersed in 20 mM Tris-HCl pH 7.6, 20 mM KCl, 1 mM $BaCl_2$, and 1 mM EDTA were mixed with detergent-solubilized MloK1 in 295 mM NaCl, 5 mM KCl, 20 mM Tris-HCl pH 8.0, 10% glycerol, 1 mM phenylmethylsulphonyl fluoride, 40/500 mM (wash/elution) imidazole, 0.2% n-decyl-β-D-maltopyranoside at LPRs ranging from 1 to 10, added to dialysis buttons sealed by a dialysis membrane with a 14-kDa molecular weight cut-off, and dialyzed for 48 h at room temperature to remove detergent. (A) Optimization of MloK1 reconstitution in liposomes by changing the LPR; although some liposomes are densely packed with MloK1, regular 2D crystalline arrays are not present. (B) Vesicular patches of MloK1 formed at an LPR of 10 and the aligned and averaged Fourier transform of the patches, indicating some weakly crystalline arrangement. Only diffraction spots up to orders (1,1) are visible above the noise. Their spacing does not agree with the crystalline arrangement obtained from planar well-ordered 2D crystals of MloK1 [98, 99], indicating that the crystal packing is different. MloK1 had an up/down alternating orientation in the latter. It might be unidirectional in the vesicular crystals as expected from the preparation method, but this remains to be shown. Scale bars: 100 nm.

[124]) from equine spleen (Figure 5A) was tested. However, urease (1 MDa [125]; diameter is 15 nm) from *Yersinia enterocolitica* bacteria (Figure 5B) was either not encapsulated or lost when the buffer was exchanged. The situation was the same for gold nanoparticles (GNPs; diameter, 5 nm) present in the encapsulation buffer alone or together with BSA. GNPs remaining in the dispersion buffer after liposome formation were not removed by ultracentrifugation (Figure 6A), but size exclusion chromatography was efficient. No GNPs were present afterwards; BSA was still encapsulated and retained as expected (Figure 6B). Interactions similar to those governing the spontaneous concentration of BSA conjugated with fluorescein (BSA-FITC [11]) and ferritin (apoferritin plus iron moiety [102]) within liposomes might have favored and/or helped to stabilize the encapsulation of BSA and apoferritin in these experiments, explaining the different result obtained with urease and GNPs. Colletier et al. investigated the encapsulation of *Drosophila melanogaster* acetylcholinesterase (AChE) in phospholipid liposomes by varying the preparation protocols, lipid composition, buffers, and ionic strengths and showed that encapsulation efficiency depends on protein-lipid bilayer interactions [62]. In particular, they suggest that stronger interaction helps to prevent loss of encapsulated material during extrusion steps and that the encapsulation of AChE is reduced in the presence of BSA because the latter competes for interaction with the phospholipids. To conclude, the many factors governing

liposome encapsulation make careful monitoring essential. Although cryo-EM is well suited to assess the encapsulation of large proteins and protein complexes, it cannot be used to follow the encapsulation of small molecules and ions.

As illustrated in Figure 7, cryo-EM is the ideal method to visualize proteoliposomes formed during the reconstitution of membrane protein oligomers and judge their quality. Both the presence of proteins densely packed in the lipid bilayer (Figure 7A) and the lattice of 2D crystals can be distinguished, allowing crystallization conditions to be optimized. Importantly, cryo-ET can be used to obtain the detailed information about the shape of vesicular 2D crystals required for image processing. The ~210-kDa protein oligomer used in the example, MloK1 [98, 99], is a bacterial potassium channel that contains S1–S4 semi-voltage sensing domains and is modulated by cAMP at its cyclic nucleotide binding domains. Three-dimensional structures were obtained at 7-Å resolution by the analysis of planar single 2D crystal layers in the presence and absence of the ligand, cAMP, by cryo-EM and electron crystallography. These structures reveal a large-scale conformational difference and indicate a possible channel gating mechanism [99]. Reconstituting MloK1 into liposomes and adding cAMP to the buffer outside of the vesicles will allow the effect of an asymmetric ligand distribution across the membrane to be investigated and compared with these results. The first step towards this is shown in Figure 7B.

9 The analysis of cryo-EM images of 2D membrane protein crystals in spherical liposomes

The formation of flat proteoliposomes filled with 2D crystals similar to those obtained for the F_0F_1 ATPase [103] is unusual as documented by negative stain electron microscopy of 2D crystallization samples; images show collapsed 2D crystal vesicles with many folds, which sometimes also have flat double-layered regions suitable for electron microscopy [98]. Thus, the challenge of analyzing 2D crystal patches in proteoliposomes of different sizes and with different degrees of sphericity must be addressed. The use of spherical or highly curved vesicles would have two advantages. First, depending on the sphericity, it might not be necessary to tilt the specimen in the microscope to obtain views of the protein in all possible orientations, as the spherical geometry will offer partial side views in the peripheral areas of a liposome image. Second, for structural studies, the protein would not have to insert in the bilayer unidirectionally; crystals with 180° screw-axis symmetry (alternating up/down protein orientations), like the p4212 planar 2D crystals formed by MloK1, would allow the 3D structures of oppositely regulated states to be determined in one experiment.

The classical image processing methods for 2D electron crystallography images, including crystal lattice unbending and Fourier filtering methods, are well established and allow access to high-resolution 3D reconstructions, when flat, well-ordered 2D crystals are available. However, they have limitations when this is not the case. One alternative approach is to treat badly ordered or non-planar 2D crystals as single particles while still exploiting the neighborhood correlation between adjacent proteins in the lattice to address the low signal-to-noise ratio of the images. This method was successfully applied to improve the resolution of the MloK1 datasets [74] and is included in the 2dx software [126, 127]. To extend this single particle approach to the analysis of 2D crystals in proteoliposomes, the algorithm would have to take into account the geometry of the liposomes and the overlapping lattices arising from crystals on both sides of them. As detailed in Jiang et al. [117], the position of a membrane protein in a spherical liposome can be directly used to determine two of the three Euler angles that define its orientation. As the sphericity of liposomes can be maintained during vitrification, this simplifies orientation determination by projection matching. The questions then are how spherical the liposomes are when 2D crystals are present in their bilayer and how regular the 2D crystals can become in the bilayer. The answers to both will depend on the protein. In molecular dynamics simulations, Parton et al. [128] demonstrate that the aggregation of α-helical membrane proteins depends on their shape, which is essentially that of a truncated cone, the curvature of the bilayer, and the hydrophobic mismatch, i.e. the difference between the length of the hydrophobic domain of the membrane protein and the length of the hydrophobic core of the lipid bilayer. Taking this a step further, empirically, the unidirectional insertion and local formation of semi-ordered 2D crystal patches of α-helical membrane proteins in a lipid bilayer should be possible for large spherical proteoliposomes, provided the correct mixture of lipids and the correct buffer conditions are used.

The presence of two layers of 2D crystals, one in the upper and one in the lower hemisphere of vesicular 2D crystals, will be visualized as two overlapping lattices in the projection images, which have to be dealt with by the image analysis software. One approach would be deconvolution of the total signal. Another would be to combine

the single particle electron crystallography approach detailed above with ET and sub-volume averaging, i.e. to use a modified form of the processing described in Jiko et al. [103] for the vesicular F_0F_1 ATPase 2D crystals. For this, the sample would have to be imaged at low dose by cryo-EM for the single particle approach and then tilted in the microscope and the same region imaged by ET, following the so-called Hagen scheme [129]. The crystal unit cell from the image recorded by single particle cryo-EM could then be located in the tomogram. A similar approach was shown to work for COPI-coated vesicles [130]. The Dynamo software system provides the necessary tools to semi-automatically pick individual 3D sub-volumes by exploiting the regular arrangement of membrane proteins in vesicular 2D crystal arrays and perform sub-tomogram averaging [96, 131].

The resolution achievable by ET and sub-volume averaging has drastically improved, and the method can now be used to reach side-chain resolution (3.9 Å) in α-helical proteins [95, 109]. Like for single particle cryo-EM, this improvement is primarily due to the increased image contrast delivered by direct electron detectors and their movie-mode imaging feature, which allows the blurring caused by beam-induced motion to be corrected.

10 Conclusions and outlook

Liposomes are widely used in science today, e.g. as models mimicking primitive cellular systems and as nanocontainers. Although they are also employed to assess the activity of membrane proteins inserted in their bilayer, they are not widely used to study the structure of these. With the technological advancement in the field, cryo-EM and cryo-ET are now in the position to rectify this. Even though the resolution for building atomic models for membrane-embedded membrane proteins is still rarely reached by these methods, the advantage of determining the structure of membrane proteins in the semi-native environment provided by a liposome bilayer must not be overlooked. Importantly, the system promises to allow structure/function relationships to be probed by introducing buffer or ligand gradients across the lipid bilayer. The snapshots obtained of the membrane proteins in action by flash-freezing at cryogenic temperatures will help to understand how they function. Further, the relatively low-resolution data can be combined with high-resolution structural models determined by other methods, if available, to enable computer modeling of protein function.

Acknowledgments: We thank ArianeFecteau-Lefebvre and Kenny Goldie for their support in data collection. This work was supported by the Swiss National Science Foundation (grants 315230_146929, 205320_144427, and the NCCR TransCure).

References

[1] Fritze A, Hens F, Kimpfler A, Schubert R, Peschka-Süss R. Remote loading of doxorubicin into liposomes driven by a transmembrane phosphate gradient. *Biochim. Biophys. Acta Biomembranes* 2006, 1758, 1633–1640.
[2] Cipolla D, Wu H, Salentinig S, Boyd B, Rades T, Vanhecke D, Petri-Fink A, Rothin-Rutishauser B, Eastman S, Redelmeier T, Gonda I, Chan HK. Formation of drug nanocrystals under nanoconfinement afforded by liposomes. *RSC Adv.* 2016, 6, 6223–6233.
[3] Chatin B, Mével M, Devallière J, Dallet L, Haudebourg T, Peuziat P, Colombani T, Berchel M, Lambert O, Edelman A, Pitard B. Liposome-based formulation for intracellular delivery of functional proteins. *Mol. Ther. Nucleic Acids* 2015, 4, e244.
[4] Forster V, Signorell RD, Roveri M, Leroux JC. Liposome-supported peritoneal dialysis for detoxification of drugs and endogenous metabolites. *Sci. Translational Med.* 2014, 6, 258ra141.
[5] Xing H, Hwang K, Lu Y. Recent developments of liposomes as nanocarriers for theranostic applications. *Theranostics* 2016, 6, 1336–1352.
[6] Liu Q, Boyd BJ. Liposomes in biosensors. *Analyst* 2013, 138, 391–409.
[7] Chen C, Wang Q. Liposome-based nanosensors for biological detection. *Am. J. Nano Res. Appl.* 2015, 3, 13–17.
[8] Yamashita Y, Oka M, Tanaka T, Yamazaki M. A new method for the preparation of giant liposomes in high salt concentrations and growth of protein microcrystals in them. *Biochim. Biophys. Acta* 2002, 1561, 129–134.
[9] de Souza TP, Fahr A, Luisi PL, Stano P. Spontaneous encapsulation and concentration of biological macromolecules in liposomes: an intriguing phenomenon and its relevance in origins of life. *J. Mol. Evol.* 2014, 79, 179–192.
[10] Cullis PR, Bally MB, Madden TD, Mayer LD, Hope MJ. pH gradients and membrane transport in liposomal systems. *Trends Biotechnol.* 1991, 9, 268–272.
[11] D'Aguanno E, Altamura E, Mavelli F, Fahr A, Stano P, Luisi PL. Physical routes to primitive cells: an experimental model based on the spontaneous entrapment of enzymes inside micrometer-sized liposomes. *Life* 2015, 5, 969–996.
[12] Rigaud JL, Levy D. Reconstitution of membrane proteins into liposomes. *Methods Enzymol.* 2003, 372, 65–86.
[13] Wang L, Tonggu L. Membrane protein reconstitution for functional and structural studies. *Sci. China Life Sci.* 2015, 58, 66–74.
[14] Mosser G. Two-dimensional crystallogenesis of transmembrane proteins. *Micron (Oxford, England: 1993)* 2001, 32, 517–540.
[15] Sachse R, Dondapati SK, Fenz SF, Schmidt T, Kubick S. Membrane protein synthesis in cell-free systems: from bio-mimetic systems to bio-membranes. *FEBS Lett.* 2014, 588, 2774–2781.

[16] Rémigy HW, Caujolle-Bert D, Suda K, Schenk A, Chami M, Engel A. Membrane protein reconstitution and crystallization by controlled dilution. *FEBS Lett.* 2003, 555, 160–169.
[17] Simeonov P, Werner S, Haupt C, Tanabe M, Bacia K. Membrane protein reconstitution into liposomes guided by dual-color fluorescence cross-correlation spectroscopy. *Biophys. Chem.* 2013, 184, 37–43.
[18] Rajendra J, Damianoglou A, Hicks M, Booth P, Rodger PM, Rodger A. Quantitation of protein orientation in flow-oriented unilamellar liposomes by linear dichroism. *Chem. Phys.* 2006, 326, 210–220.
[19] Islam ST, Eckford PD, Jones ML, Nugent T, Bear CE, Vogel C, Lam JS. Proton-dependent gating and proton uptake by Wzx support O-antigen-subunit antiport across the bacterial inner membrane. *MBio* 2013, 4, e00678–00613.
[20] Tunuguntla R, Bangar M, Kim K, Stroeve P, Ajo-Franklin CM, Noy A. Lipid bilayer composition can influence the orientation of proteorhodopsin in artificial membranes. *Biophys. J.* 2013, 105, 1388–1396.
[21] Neves P, Lopes SC, Sousa I, Garcia S, Eaton P, Gameiro P. Characterization of membrane protein reconstitution in LUVs of different lipid composition by fluorescence anisotropy. *J. Pharm. Biomed. Anal.* 2009, 49, 276–281.
[22] Dezi M, Di Cicco A, Bassereau P, Levy D. Detergent-mediated incorporation of transmembrane proteins in giant unilamellar vesicles with controlled physiological contents. *Proc. Natl Acad. Sci. USA* 2013, 110, 7276–7281.
[23] Rigaud JL. Membrane proteins: functional and structural studies using reconstituted proteoliposomes and 2-D crystals. *Brazilian J. Med. Biol. Res.* 2002, 35, 753–766.
[24] Das BB, Lu GJ, Son WS, Tian Y, Marassi FM, Opella SJ. Structure determination of a membrane protein in proteoliposomes. *J. Am. Chem. Soc.* 2012, 134, 2047–2056.
[25] Almgren M, Edwards K, Karlsson G. Cryo transmission electron microscopy of liposomes and related structures. *Colloids Surf. A* 2000, 174, 3–21.
[26] Egerdie B, Singer M. Morphology of gel state phosphatidylethanolamine and phosphatidylcholine liposomes: a negative stain electron microscopic study. *Chem. Phys. Lipids* 1982, 31, 75–85.
[27] Thompson AK, Mozafari MR, Singh H. The properties of liposomes produced from milk fat globule membrane material using different techniques. *Lait* 2007, 87, 349–360.
[28] Stokes DL, Rice WJ, Hu M, Kim C, Ubarretxena I. Two-dimensional crystallization of integral membrane proteins for electron crystallography. *Methods Mol. Biol. (Clifton, N.J.)* 2010, 654, 187–205.
[29] Vink M, Derr K, Love J, Stokes DL, Ubarretxena-Belandia I. A high-throughput strategy to screen 2D crystallization trials of membrane proteins. *J. Struct. Biol.* 2007, 160, 295–304.
[30] Gonen T, Cheng Y, Sliz P, Hiroaki Y, Fujiyoshi Y, Harrison SC, Walz T. Lipid-protein interactions in double-layered two-dimensional AQP0 crystals. *Nature* 2005, 438, 633–638.
[31] Walz T, Smith BL, Zeidel ML, Engel A, Agre P. Biologically active two-dimensional crystals of aquaporin CHIP. *J. Biol. Chem.* 1994, 269, 1583–1586.
[32] Ohsawa T, Miura H, Harada K. Studies on the effect of water-soluble additives and on the encapsulation mechanism in liposome preparation by the freeze-thawing method. *Chem. Pharm. Bull.* 1985, 33, 5474–5483.
[33] Dubochet J, Adrian M, Chang JJ, Homo JC, Lepault J, McDowall AW, Schultz P. Cryo-electron microscopy of vitrified specimens. *Q. Rev. Biophys.* 1988, 21, 129–228.
[34] Medalia O, Weber I, Frangakis AS, Nicastro D, Gerisch G, Baumeister W. Macromolecular architecture in eukaryotic cells visualized by cryoelectron tomography. *Science (New York, N.Y.)* 2002, 298, 1209–1213.
[35] Bonnaud C, Monnier CA, Demurtas D, Jud C, Vanhecke D, Montet X, Hovius R, Lattuada M, Rothen-Rutishauser B, Petri-Fink A. Insertion of nanoparticle clusters into vesicle bilayers. *ACS Nano* 2014, 8, 3451–3460.
[36] Rangelov S, Edwards K, Almgren M, Karlsson G. Steric stabilization of egg-phosphatidylcholine liposomes by copolymers bearing short blocks of lipid-mimetic units. *Langmuir ACS J. Surf. Colloids* 2003, 19, 172–181.
[37] Le Bihan O, Bonnafous P, Marak L, Bickel T, Trépout S, Mornet S, De Haas F, Talbot H, Taveau JC, Lambert O. Cryo-electron tomography of nanoparticle transmigration into liposome. *J. Struct. Biol.* 2009, 168, 419–425.
[38] Sborgi L, Rühl S, Mulvihill E, Pipercevic J, Heilig R, Stahlberg H, Farady CJ, Müller DJ, Broz P, Hiller S. GSDMD membrane pore formation constitutes the mechanism of pyroptotic cell death. *EMBO J.* 2016, 35, 1766–1778.
[39] Zhang M, Charles R, Tong H, Zhang L, Patel M, Wang F, Rames MJ, Ren A, Rye KA, Qiu X, Johns DG, Charles MA, Ren G. HDL surface lipids mediate CETP binding as revealed by electron microscopy and molecular dynamics simulation. *Sci. Rep.* 2015, 5, 8741.
[40] Fox CB, Mulligan SK, Sung J, Dowling QM, Fung HW, Vedvick TS, Coler RN. Cryogenic transmission electron microscopy of recombinant tuberculosis vaccine antigen with anionic liposomes reveals formation of flattened liposomes. *Int. J. Nanomed.* 2014, 9, 1367–1377.
[41] Milanesi L, Sheynis T, Xue WF, Orlova EV, Hellewell AL, Jelinek R, Hewitt EW, Radford SE, Saibil HR. Direct three-dimensional visualization of membrane disruption by amyloid fibrils. *Proc. Natl. Acad. Sci. USA* 2012, 109, 20455–20460.
[42] Stewart PL. Cryo-electron microscopy and cryo-electron tomography of nanoparticles. *Wiley interdisciplinary reviews. Nanomed. Nanobiotechnol.* 2016, in press.
[43] Fagerberg L, Jonasson K, von Heijne G, Uhlen M, Berglund L. Prediction of the human membrane proteome. *Proteomics* 2010, 10, 1141–1149.
[44] Fontanesi F. 2015. Mitochondria: structure and role in respiration. *eLS*. 1–13. DOI: 10.1002/9780470015902.a0001380.pub2
[45] Goni FM. The basic structure and dynamics of cell membranes: an update of the Singer-Nicolson model. *Biochim. Biophys. Acta* 2014, 1838, 1467–1476.
[46] Arinaminpathy Y, Khurana E, Engelman DM, Gerstein MB. Computational analysis of membrane proteins: the largest class of drug targets. *Drug Discovery Today* 2009, 14, 1130–1135.
[47] Renault L, Chou HT, Chiu PL, Hill RM, Zeng X, Gipson B, Zhang ZY, Cheng A, Unger V, Stahlberg H. Milestones in electron crystallography. *J. Comput. Aided Mol. Des.* 2006, 20, 519–527.
[48] Abe K, Fujiyoshi Y. Cryo-electron microscopy for structure analyses of membrane proteins in the lipid bilayer. *Curr. Opin. Struct. Biol.* 2016, 39, 71–78.
[49] Stahlberg H, Biyani N, Engel A. 3D reconstruction of two-dimensional crystals. *Arch. Biochem. Biophys.* 2015, 581, 68–77.

[50] Banerjee RK, Datta AG. Proteoliposome as the model for the study of membrane-bound enzymes and transport proteins. *Mol. Cell Biochem.* 1983, 50, 3–15.
[51] Phillips R, Ursell T, Wiggins P, Sens P. Emerging roles for lipids in shaping membrane-protein function. *Nature* 2009, 459, 379–385.
[52] Pekker M, Shneider MN. The surface charge of a cell lipid membrane. *ArXiv e-prints* 2014, arXiv:1401.4707.
[53] Bezanilla F. How membrane proteins sense voltage. *Nat. Rev. Mol. Cell Biol.* 2008, 9, 323–332.
[54] Akbarzadeh A, Rezaei-Sadabady R, Davaran S, Joo SW, Zarghami N, Hanifehpour Y, Samiei M, Kouhi M, Nejati-Koshki K. Liposome: classification, preparation, and applications. *Nanoscale Res. Lett.* 2013, 8, 102–102.
[55] Huang Y, Hemmer E, Rosei F, Vetrone F. Multifunctional liposome nanocarriers combining upconverting nanoparticles and anticancer drugs. *J. Phys. Chem. B* 2016, 120, 4992–5001.
[56] Yu B, Lee RJ, Lee LJ. Microfluidic methods for production of liposomes. *Methods Enzymol.* 2009, 465, 129–141.
[57] Craig LC, Gregory JD, Hausmann W. Versatile laboratory concentration device. *Anal. Chem.* 1950, 22, 1462.
[58] Mayer LD, Hope MJ, Cullis PR. Vesicles of variable sizes produced by a rapid extrusion procedure. *Biochim. Biophys. Acta Biomembranes* 1986, 858, 161–168.
[59] MacDonald RC, MacDonald RI, Menco BPM, Takeshita K, Subbarao NK, Hu L-r. Small-volume extrusion apparatus for preparation of large, unilamellar vesicles. *Biochim. Biophys. Acta Biomembranes* 1991, 1061, 297–303.
[60] Hinna A, Steiniger F, Hupfeld S, Stein P, Kuntsche J, Brandl M. Filter-extruded liposomes revisited: a study into size distributions and morphologies in relation to lipid-composition and process parameters. *J. Liposome Res.* 2016, 26, 11–20.
[61] Mui B, Chow L, Hope MJ. Extrusion technique to generate liposomes of defined size. *Methods Enzymol.* 2003, 367, 3–14.
[62] Colletier J-P, Chaize B, Winterhalter M, Fournier D. Protein encapsulation in liposomes: efficiency depends on interactions between protein and phospholipid bilayer. *BMC Biotechnol.* 2002, 2, 9.
[63] Schwille P. Giant unilamellar vesicles: from minimal membrane systems to minimal cells? In *The Minimal Cell: The Biophysics of Cell Compartment and the Origin of Cell Functionality* (eds Luisi LP, Stano P). Springer, Netherlands, 2011.
[64] Morales-Penningston NF, Wu J, Farkas ER, Goh SL, Konyakhina TM, Zheng JY, Webb WW, Feigenson GW. GUV preparation and imaging: minimizing artifacts. *Biochim. Biophys. Acta* 2010, 1798, 1324–1332.
[65] Stockbridge RB, Tsai MF. Lipid reconstitution and recording of recombinant ion channels. *Methods Enzymol.* 2015, 556, 385–404.
[66] Kühlbrandt W. Two-dimensional crystallization of membrane proteins: a practical guide. In: *Membrane protein purification and crystallization: a practical guide,* Hunte, C., Jagow, G. von, Schägger, H. eds., 2nd edition, Academic Press: San Diego, 2003, 253–284.
[67] Rigaud JL, Mosser G, Lacapere JJ, Olofsson A, Levy D, Ranck JL. Bio-Beads: an efficient strategy for two-dimensional crystallization of membrane proteins. *J. Struct. Biol.* 1997, 118, 226–235.
[68] Signorell GA, Kaufmann TC, Kukulski W, Engel A, Remigy HW. Controlled 2D crystallization of membrane proteins using methyl-beta-cyclodextrin. *J. Struct. Biol.* 2007, 157, 321–328.
[69] Abeyrathne PD, Arheit M, Kebbel F, Castano-Diez D, Goldie KN, Chami M, Stahlberg H, Renault L, Kühlbrandt W. 1.15 Analysis of 2-D crystals of membrane proteins by electron microscopy A2 – Egelman, Edward H. In *Comprehensive Biophysics*. Elsevier, 2012.
[70] Glaves JP, Fisher L, Ward A, Young HS. Helical crystallization of two example membrane proteins MsbA and the Ca(2+)-ATPase. *Methods Enzymol.* 2010, 483, 143–159.
[71] Korkhov VM, Sachse C, Short JM, Tate CG. Three-dimensional structure of TspO by electron cryomicroscopy of helical crystals. *Structure (London, England: 1993)* 2010, 18, 677–687.
[72] Kuang Q, Purhonen P, Hebert H. Two-dimensional crystallization procedure, from protein expression to sample preparation. *BioMed Res. Int.* 2015, 2015, 693869.
[73] Schenk AD, Castano-Diez D, Gipson B, Arheit M, Zeng X, Stahlberg H. 3D econstruction from 2D crystal image and diffraction data. *Methods Enzymol.* 2010, 482, 101–129.
[74] Scherer S, Arheit M, Kowal J, Zeng X, Stahlberg H. Single particle 3D reconstruction for 2D crystal images of membrane proteins. *J. Struct. Biol.* 2014, 185, 267–277.
[75] Sachse C, Chen JZ, Coureux PD, Stroupe ME, Fandrich M, Grigorieff N. High-resolution electron microscopy of helical specimens: a fresh look at tobacco mosaic virus. *J. Mol. Biol.* 2007, 371, 812–835.
[76] Whittaker JW. Cell-free protein synthesis: the state of the art. *Biotechnol. Lett.* 2013, 35, 143–152.
[77] Rosenblum G, Cooperman BS. Engine out of the chassis: cell-free protein synthesis and its uses. *FEBS Lett.* 2014, 588, 261–268.
[78] Niwa T, Sasaki Y, Uemura E, Nakamura S, Akiyama M, Ando M, Sawada S, Mukai SA, Ueda T, Taguchi H, Akiyoshi K. Comprehensive study of liposome-assisted synthesis of membrane proteins using a reconstituted cell-free translation system. *Sci. Rep.* 2015, 5, 18025.
[79] Katzen F, Peterson TC, Kudlicki W. Membrane protein expression: no cells required. *Trends Biotechnol.* 2009, 27, 455–460.
[80] Yang Y, Wang J, Shigematsu H, Xu W, Shih WM, Rothman JE, Lin C. Self-assembly of size-controlled liposomes on DNA nanotemplates. *Nat. Chem.* 2016, 8, 476–483.
[81] Long AR, O'Brien CC, Alder NN. The cell-free integration of a polytopic mitochondrial membrane protein into liposomes occurs cotranslationally and in a lipid-dependent manner. *PloS one* 2012, 7, e46332.
[82] Mondal S, Johnston JM, Wang H, Khelashvili G, Filizola M, Weinstein H. Membrane driven spatial organization of GPCRs. *Sci. Rep.* 2013, 3, 2909.
[83] Hite RK, Gonen T, Harrison SC, Walz T. Interactions of lipids with aquaporin-0 and other membrane proteins. *Pflugers Archiv. Eur. J. Physiol.* 2008, 456, 651–661.
[84] Seddon AM, Curnow P, Booth PJ. Membrane proteins, lipids and detergents: not just a soap opera. *Biochim. Biophys. Acta Biomembranes* 2004, 1666, 105–117.
[85] Pantelic RS, Suk JW, Hao Y, Ruoff RS, Stahlberg H. Oxidative doping renders graphene hydrophilic, facilitating its use as a support in biological TEM. *Nano Lett.* 2011, 11, 4319–4323.
[86] Pantelic RS, Suk JW, Magnuson CW, Meyer JC, Wachsmuth P, Kaiser U, Ruoff RS, Stahlberg H. Graphene: substrate preparation and introduction. *J. Struct. Biol.* 2011, 174, 234–238.
[87] Pantelic RS, Meyer JC, Kaiser U, Baumeister W, Plitzko JM. Graphene oxide: a substrate for optimizing preparations of frozen-hydrated samples. *J. Struct. Biol.* 2010, 170, 152–156.
[88] Razinkov I, Dandey VP, Wei H, Zhang Z, Melnekoff D, Rice WJ, Wigge C, Potter CS, Carragher B. A new method for vitrifying samples for cryoEM. *J. Struct. Biol.* 2016, 195, 190–198.

[89] Arnold SA, Albiez S, Bieri A, Syntychaki A, Adaixo R, McLeod RA, Goldie KN, Stahlberg H, Braun T. Blotting-free and loss-less cryo-electron microscopy grid preparation from nanoliter-sized protein samples. *J. Struct. Biol.* 2017, in press.
[90] Li X, Mooney P, Zheng S, Booth CR, Braunfeld MB, Gubbens S, Agard DA, Cheng Y. Electron counting and beam-induced motion correction enable near-atomic-resolution single-particle cryo-EM. *Nature methods* 2013, 10, 584–590.
[91] Brilot AF, Chen JZ, Cheng A, Pan J, Harrison SC, Potter CS, Carragher B, Henderson R, Grigorieff N. Beam-induced motion of vitrified specimen on holey carbon film. *J. Struct. Biol.* 2012, 177, 630–637.
[92] McLeod R, Kowal J, Ringler P, Stahlberg H. Zorro: robust image alignment for cryogenic transmission electron microscopy. *J. Struct. Biol.* 2017, in press.
[93] Carazo JM, Sorzano COS, Otón J, Marabini R, Vargas J. Three-dimensional reconstruction methods in single particle analysis from transmission electron microscopy data. *Arch. Biochem. Biophys.* 2015, 581, 39–48.
[94] Al-Amoudi A, Chang JJ, Leforestier A, McDowall A, Salamin LM, Norlén LP, Richter K, Blanc NS, Studer D, Dubochet J. Cryo-electron microscopy of vitreous sections. *EMBO J.* 2004, 23, 3583–3588.
[95] Bharat TA, Russo CJ, Lowe J, Passmore LA, Scheres SH. Advances in single-particle electron cryomicroscopy structure determination applied to sub-tomogram averaging. *Structure (London, England: 1993)* 2015, 23, 1743–1753.
[96] Castano-Diez D, Kudryashev M, Arheit M, Stahlberg H. Dynamo: a flexible, user-friendly development tool for subtomogram averaging of cryo-EM data in high-performance computing environments. *J. Struct. Biol.* 2012, 178, 139–151.
[97] Thompson RF, Walker M, Siebert CA, Muench SP, Ranson NA. An introduction to sample preparation and imaging by cryo-electron microscopy for structural biology. *Methods* 2016, 100, 3–15.
[98] Chiu P-L, Pagel MD, Evans J, Chou HT, Zeng X, Gipson B, Stahlberg H, Nimigean CM. The structure of the prokaryotic cyclic nucleotide-modulated potassium channel MloK1 at 16 Å resolution. *Structure (London, England: 1993)* 2007, 15, 1053–1064.
[99] Kowal J, Chami M, Baumgartner P, Arheit M, Chiu PL, Rangl M, Scheuring S, Schröder GF, Nimigean CM, Stahlberg H. Ligand-induced structural changes in the cyclic nucleotide-modulated potassium channel MloK1. *Nat. Commun.* 2014, 5, 3106.
[100] Evjen TJ, Hupfeld S, Barnert S, Fossheim S, Schubert R, Brandl M. Physicochemical characterization of liposomes after ultrasound exposure – mechanisms of drug release. *J. Pharm. Biomed. Anal.* 2013, 78–79, 118–122.
[101] Kuntsche J, Horst JC, Bunjes H. Cryogenic transmission electron microscopy (cryo-TEM) for studying the morphology of colloidal drug delivery systems. *Int. J. Pharm.* 2011, 417, 120–137.
[102] Pereira de Souza T, Steiniger F, Stano P, Fahr A, Luisi PL. Spontaneous crowding of ribosomes and proteins inside vesicles: a possible mechanism for the origin of cell metabolism. *Chembiochem Eur J. Chem. Biol.* 2011, 12, 2325–2330.
[103] Jiko C, Davies KM, Shinzawa-Itoh K, Tani K, Maeda S, Mills DJ, Tsukihara T, Fujiyoshi Y, Kühlbrandt W, Gerle C. Bovine F(1)F(o) ATP synthase monomers bend the lipid bilayer in 2D membrane crystals. *eLife* 2015, 4, e06119.
[104] Helmprobst F, Frank M, Stigloher C. Presynaptic architecture of the larval zebrafish neuromuscular junction. *J. Comp. Neurol.* 2015, 523, 1984–1997.
[105] Irobalieva RN, Martins B, Medalia O. Cellular structural biology as revealed by cryo-electron tomography. *J. Cell Sci.* 2016, 129, 469.
[106] Jasnin M, Ecke M, Baumeister W, Gerisch G. Actin organization in cells responding to a perforated surface, revealed by live imaging and cryo-electron tomography. *Structure (London, England: 1993)* 2016, 24, 1031–1043.
[107] Bitto D, Halldorsson S, Caputo A, Huiskonen JT. Low pH and anionic lipid-dependent fusion of *Uukuniemi* phlebovirus to liposomes. *J. Biol. Chem.* 2016, 291, 6412–6422.
[108] Strauss JD, Hammonds JE, Yi H, Ding L, Spearman P, Wright ER. Three-dimensional structural characterization of HIV-1 tethered to human cells. *J. Virol.* 2016, 90, 1507–1521.
[109] Schur FK, Obr M, Hagen WJ, Wan W, Jakobi AJ, Kirkpatrick JM, Sachse C, Kräusslich HG, Briggs JA. An atomic model of HIV-1 capsid-SP1 reveals structures regulating assembly and maturation. *Science (New York, N.Y.)* 2016, 353, 506–508.
[110] Kudryashev M, Diepold A, Amstutz M, Armitage JP, Stahlberg H, Cornelis GR. *Yersinia enterocolitica* type III secretion injectisomes form regularly spaced clusters, which incorporate new machines upon activation. *Mol. Microbiol.* 2015, 95, 875–884.
[111] Menzel K, Apfel UP, Wolter N, Rüger R, Alpermann T, Steiniger F, Gabel D, Förster S, Weigand W, Fahr A. [FeFe]-hydrogenase models assembled into vesicular structures. *J. Liposome Res.* 2014, 24, 59–68.
[112] Kim J, Wu S, Tomasiak TM, Mergel C, Winter MB, Stiller SB, Robles-Colmanares Y, Stroud RM, Tampé R, Craik CS, Cheng Y. Subnanometre-resolution electron cryomicroscopy structure of a heterodimeric ABC exporter. *Nature* 2015, 517, 396–400.
[113] Popot JL. Amphipols, nanodiscs, and fluorinated surfactants: three nonconventional approaches to studying membrane proteins in aqueous solutions. *Annu. Rev. Biochem.* 2010, 79, 737–775.
[114] Gao Y, Cao E, Julius D, Cheng Y. TRPV1 structures in nanodiscs reveal mechanisms of ligand and lipid action. *Nature* 2016, 534, 347–351.
[115] Liao M, Cao E, Julius D, Cheng Y. Structure of the TRPV1 ion channel determined by electron cryo-microscopy. *Nature* 2013, 504, 107–112.
[116] Vinothkumar KR. Membrane protein structures without crystals, by single particle electron cryomicroscopy. *Curr. Opin. Struct. Biol.* 2015, 33, 103–114.
[117] Jiang QX, Chester DW, Sigworth FJ. Spherical reconstruction: a method for structure determination of membrane proteins from cryo-EM images. *J. Struct. Biol.* 2001, 133, 119–131.
[118] Wang L, Sigworth FJ. Liposomes on a streptavidin crystal: a system to study membrane proteins by cryo-EM. *Methods Enzymol.* 2010, 481, 147–164.
[119] Liu Y, Sigworth FJ. Automatic cryo-EM particle selection for membrane proteins in spherical liposomes. *J. Struct. Biol.* 2014, 185, 295–302.
[120] Basta T, Wu HJ, Morphew MK, Lee J, Ghosh N, Lai J, Heumann JM, Wang K, Lee YC, Rees DC, Stowell MH. Self-assembled lipid and membrane protein polyhedral nanoparticles. *Proc. Natl Ac. Sci. USA* 2014, 111, 670–674.
[121] Kudryashev M, Castaño-Díez D, Deluz C, Hassaine G, Grasso L, Graf-Meyer A, Vogel H, Stahlberg H. The structure of the

mouse serotonin 5-HT3 receptor in lipid vesicles. *Structure (London, England: 1993)* 2016, 24, 165–170.
[122] Garcia-Manyes S, Oncins G, Sanz F. Effect of ion-binding and chemical phospholipid structure on the nanomechanics of lipid bilayers studied by force spectroscopy. *Biophys. J.* 2005, 89(3), 1812–1826.
[123] Xia S, Xu S. Ferrous sulfate liposomes: preparation, stability and application in fluid milk. *Food Res. Int.* 2005, 38, 289–296.
[124] Kim M, Rho Y, Jin KS, Ahn B, Jung S, Kim H, Ree M. pH-Dependent structures of ferritin and apoferritin in solution: disassembly and reassembly. *Biomacromolecules* 2011, 12, 1629–1640.
[125] Bhagat N, Virdi JS. Molecular and biochemical characterization of urease and survival of *Yersinia enterocolitica* biovar 1A in acidic pH *in vitro*. *BMC Microbiol.* 2009, 9, 1–14.
[126] Gipson B, Zeng X, Zhang ZY, Stahlberg H. 2dx--user-friendly image processing for 2D crystals. *J. Struct. Biol.* 2007, 157, 64–72.
[127] Arheit M, Castaño-Díez D, Thierry R, Gipson BR, Zeng X, Stahlberg H. Image processing of 2D crystal images. *Methods Mol. Biol.* 2013, 955, 171–194.
[128] Parton Daniel L, Klingelhoefer Jochen W, Sansom Mark SP. Aggregation of model membrane proteins, modulated by hydrophobic mismatch, membrane curvature, and protein class. *Biophys. J.* 2011, 101, 691–699.
[129] Hagen WJ, Wan W, Briggs JA. Implementation of a cryo-electron tomography tilt-scheme optimized for high resolution subtomogram averaging. *J. Struct. Biol.* 2016, in press.
[130] Faini M, Prinz S, Beck R, Schorb M, Riches JD, Bacia K, Brügger B, Wieland FT, Briggs JA. The structures of COPI-coated vesicles reveal alternate coatomer conformations and interactions. *Science (New York, N.Y.)* 2012, 336, 1451–1454.
[131] Castano-Diez D, Kudryashev M, Stahlberg H. Dynamo catalogue: geometrical tools and data management for particle picking in subtomogram averaging of cryo-electron tomograms. *J. Struct. Biol.* 2016, in press.

Bionotes

Kushal Sejwal
Center for Cellular Imaging and NanoAnalytics (C-CINA), Biozentrum, University of Basel, Basel 4056, Switzerland

Kushal Sejwal received his BS in Life Sciences from the University of Delhi and MS in Bioinformatics from Jamia Millia Islamia, New Delhi, India. He worked as a research associate at the Rudolf Virchow Center, University of Würzburg, in Germany for 2 years, where he was first introduced to the field of cryo-electron microscopy. In October 2012, he moved to Basel, Switzerland, to pursue a PhD in the laboratory of Prof. Henning Stahlberg at the C-CINA, Biozentrum, University of Basel. He worked on structural elucidation of macromolecular complexes by cryo-EM and method development using proteoliposomes. In August 2016, he finished his PhD and started his postdoctoral training in the laboratory of Prof. Michel Steinmetz at the Paul Scherrer Institute in Switzerland.

Mohamed Chami
Center for Cellular Imaging and NanoAnalytics (C-CINA), Biozentrum, University of Basel, Basel 4056, Switzerland

Mohamed Chami obtained his undergraduate degree in biology and geology at the University of Oujda in Morocco. After receiving a master's degree in biochemistry in 1994 from the University of Paris, France, he pursued a PhD on the structure of the cell envelope of *Corynebacterium glutamicum* at the same University. From 1999 to 2003, he worked as a post-doc on reconstitution and 2D crystallization of membrane proteins in the group of Jean-Louis Rigaud at the Institut Curie in Paris. He moved to Basel, Switzerland, in 2003 and worked until 2008 in the laboratory of Andreas Engel and, since 2009, in the laboratory of Henning Stahlberg as a senior scientist, where he is involved in the structure elucidation of membrane proteins using cryo-electron microscopy. Since January 2016, Dr. Chami had been directing the BioEM laboratory, the service facility for electron microscopy in the life sciences at the Biozentrum of the University of Basel, Switzerland.

Julia Kowal
Center for Cellular Imaging and NanoAnalytics (C-CINA), Biozentrum, University of Basel, Basel 4056, Switzerland

Julia Kowal from Poland got her master's degree in biochemistry at the Jagiellonian University, Kraków, Poland, and then obtained her PhD in biophysics in the group of Prof. Andreas Engel at the University of Basel, Switzerland. She then studied potassium channel structures by cryo-electron microscopy in the group of Prof. Stahlberg at C-CINA from 2011 to 2016. Since 2016, she has been a post-doc in the group of Prof. Locher at the ETH Zurich, Switzerland, where she continues studying membrane proteins by cryo-electron microscopy.

Shirley A. Müller
Center for Cellular Imaging and NanoAnalytics (C-CINA), Biozentrum, University of Basel, Basel 4056, Switzerland

Shirley A. Müller received a PhD in Chemistry from the University of Exeter, UK, in 1977. Since then, the main focus of her scientific career has been mass measurements by scanning transmission electron microscopy, in the group of Andreas Engel at the Maurice E. Müller Institute for High-Resolution Electron Microscopy and at C-CINA (both at the Biozentrum, University of Basel, Switzerland). Her present tasks at C-CINA in the group of Henning Stahlberg are concerned with project management and scientific editing.

Henning Stahlberg
Center for Cellular Imaging and NanoAnalytics (C-CINA), Biozentrum, University of Basel, Basel 4056, Switzerland,
henning.stahlberg@unibas.ch.
http://orcid.org/0000-0002-1185-4592

Henning Stahlberg studied physics at the Technical University of Berlin, Germany, from 1989 to 1992, and obtained his PhD from 1992 to 1997 in structural biology of membrane proteins at the EPFL in Lausanne, Switzerland, in the groups of Prof. Dubochet and Vogel. From 1998 to 2003, he studied membrane proteins by cryo-electron microscopy as a post-doc in the group of Prof. Engel at the Biozentrum, University of Basel, Switzerland. In 2003, he joined the University of California in Davis, CA, USA, as Assistant Professor, where he became tenured Associate Professor in 2007. Since 2009, he has been directing the Center for Cellular Imaging and NanoAnalytics (C-CINA) as Professor of the Biozentrum at the University of Basel, Switzerland.